Desalination and Water Treatment
www.deswater.com

doi: 10.1080/19443994.2016.1143878

57 (2016) 24925–24933
November

Taylor & Francis
Taylor & Francis Group

Film pore diffusion modeling and contact time optimization for adsorption of distillery spentwash on fly ash

D. Aravind, R. Krishna Prasad*

Department of Chemical Engineering and Materials Science, Amrita Vishwa Vidyapeetham University, Ettimadai, Coimbatore 641 112, India, Tel. +91 422 268500; Fax: +91 422 2656274; emails: aravind.devanand@gmail.com (D. Aravind), rkprasad_cbe@rediffmail.com (R. Krishna Prasad)

Received 23 March 2015; Accepted 12 January 2016

ABSTRACT

The contact time in two batch adsorbers were optimized using unreacted shrinking core model for the adsorption of biopolymeric pigments in distillery spentwash by fly ash adsorbent. The total optimal contact time obtained was 40 min for 3 m^3 adsorbate volume having initial biopolymer concentration of 1.5 mg/dm^3. The film pore diffusion model was used to determine the external mass transfer coefficient, effective diffusion coefficient, and bed capacity for continuous adsorption process. The adsorbent bed capacities at different initial biopolymeric concentrations (2,000, 5,500, 8,700, and 12,500 mg/ml) are 69.26, 114.41, 143.64, and 172 mg/g, respectively. The effective diffusion coefficients at various bed heights were determined for continuous adsorption process.

Keywords: Distillery spentwash; Fly ash; Film pore diffusion model; Adsorption; Contact time optimization

1. Introduction

The adsorption is a physiochemical process used in industrial effluent treatment. In adsorption process the solute particles are attached to the adsorbent surface by physical or chemical bonds. The amount of feed charged to the batch adsorber is fixed but in dynamic adsorber feed supply is continuous at constant flow rate [1]. The molasses spentwash obtained from distill units of distillery has melanoidin biopolymeric pigments formed due to Maillard amino carbonyl reaction which exists in dark brown color in the effluent. The empirical formula of this pigment is $C_{17–18}H_{26–27}$ O_{10} N and molecular weight is in the range of 5,000–40,000 [2]. The adsorption is widely used in textile and distillery industries to remove color, suspended particles, and to reduce chemical oxygen demand (COD) from waste effluent [3]. The other techniques like biological treatment and advanced oxidation techniques are also used in effluent treatment processes [4]. The fly ash discarded from coal power stations is used as adsorbent to remove the melanoidin pigments from distillery spentwash as it has good adsorption capacity [5–7]. The fly ash is used as adsorbent to remove chromium, copper, zinc, and arsenic [8].

The design parameters of adsorption column are determined experimentally or predicted through mathematical models. The adsorption kinetics and equilibrium data are essential to develop mathematical models for adsorption systems. The film pore diffusion model was used to study the adsorption of distillery

*Corresponding author.

spentwash on fly ash based on unreacted shrinking core model principles. This model assumes the adsorbent as solid with small pores in which adsorbate is attached and this model is applicable for irreversible adsorption at high solid to liquid solute distributions. The diffusion of solute into adsorbent occurs according to the Fick's law of diffusion [9]. This model was successfully applied to many systems like dyestuffs adsorption using activated carbon and charred saw dust [10–12], adsorption of dye stuffs from aqueous solution [13,14], and protein adsorption [15].

The major impurity in spentwash is biopolymeric melanoidin pigment composed of highly dispersed colloids [16]. Many methods like employing bacteria [17], electrochemical methods [18], coagulating techniques [19], and adsorption [20] are currently used for removing this pigment. The film pore diffusion model was used to optimize the contact time of batch adsorbers and to estimate various adsorption parameters for adsorption of distillery spentwash in fly ash.

2. Materials and methods

The molasses spentwash was obtained from a distillery unit near Tiruchi, Tamil Nadu. The pH adjustment in the sample was done using 0.1 M H_2SO_4 or 0.1 M NaOH as per the requirement. The fly ash from a thermal power plant was sieved and collected in the range of BSS # –72 + 100, –100 + 150, –150 + 200, and –200 + 300 mesh size with average particle diameter 0.1815, 0.128, 0.09, and 0.071 mm respectively.

The batch adsorption studies were conducted at 293, 303, and 313 K by adding appropriate dosage of fly ash adsorbent to 100 ml distillery spentwash agitated at 200 rpm in an incubated shaker for 3 h. The analysis of sample was done after filtering in Whatman 42 filter paper. The absorbance of sample at characteristic wavelength of 475 nm was determined using double beam UV–vis spectrophotometer (Systronics 2201) [21]. The readings were taken in duplicate for each sample to check repeatability and the average values were recorded.

Percentage color removal (R_t) was calculated using the formula:

$$\%R_t = \frac{C_o - C_t}{C_o} \times 100 \quad (1)$$

Specific uptake was calculated by:

$$q_t = \frac{C_o - C_t}{m_s} \quad (2)$$

The packed bed adsorber with BSS # –100 + 150 mesh size fly ash particles was used to remove melanoidin pigments in spentwash. The glass column with internal diameter of 2 cm with five sampling points at 5 cm intervals was packed with glass beads of 3 mm diameter for 2 cm height at the bottom to provide uniform inlet flow to the column. The experiments with spentwash sample at pH 7 having initial concentration 2,000 mg/L were conducted at different flow rates (1, 2, and 3 L/h) supplied using peristaltic pump on 10 cm bed height.

3. Results and discussions

3.1. Studies on effect of initial concentration of solute on solid-phase adsorbent uptake

The Langmuir isotherm model used to predict the solid-phase adsorbent concentration at different temperatures is given below:

$$q_{e,t} = \frac{K_L C_{e,t}}{1 + a_L C_{e,t}} \quad (3)$$

It can be observed from Fig. 1 that the equilibrium uptake of adsorbent increases with increase in solution concentration. The adsorbent concentration reaches a saturation point beyond which the solution concentration has no significant effect on the adsorbent concentration. The adsorption is an exothermic process and by the Lechatlier's principle an increase in temperature will favor desorption process and hence the temperature has an inverse effect on adsorbent concentration. The maximum value of the solid-phase

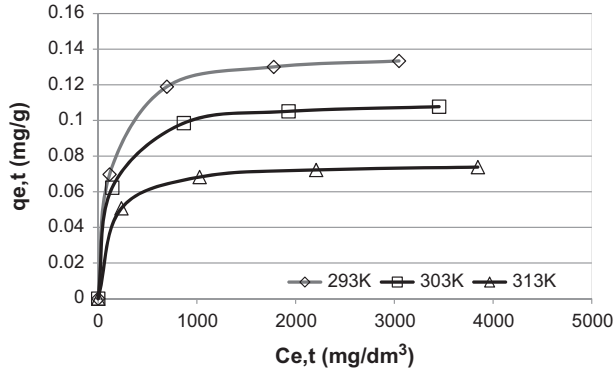

Fig. 1. Predicted q_e for different temperatures of batch adsorption studies using Langmuir isotherm.
Notes: Conditions: pH 7, particle size BSS # –150 + 200, dosage = 10 g, time = 150 min.

concentration was 0.133 mg/g at 293 K. The treatment of 10% diluted sample of distillery spentwash with 10 g of fly ash adsorbent at different temperatures to measure the percentage of spentwash remaining is shown in Fig. 2.

3.2. Modified Langmuir isotherm model

The model equation for the modified Langmuir isotherm is given below:

$$q_e = \frac{bT^{-n} C_e}{1 + bC_e} \quad (4)$$

In this model b and n are isotherm constants that consider the energy of adsorption. The theoretical values of q_e and C_e were fitted to this model to determine the parameters b and n. The Langmuir isotherm cannot be used as such for adsorption from solution because of simultaneous adsorption and desorption of different species for balancing the energy and mass and it assumes homogeneity of adsorption surface which is not valid for adsorption from solution [22,23]. The modified Langmuir isotherm considers the change in free energy of adsorption with temperature. The variation in concentration of solute with specific uptake is provided for different temperatures in Fig. 3. The corresponding predicted models of modified Langmuir isotherm are tabulated for different temperatures of adsorption operation in Table 1.

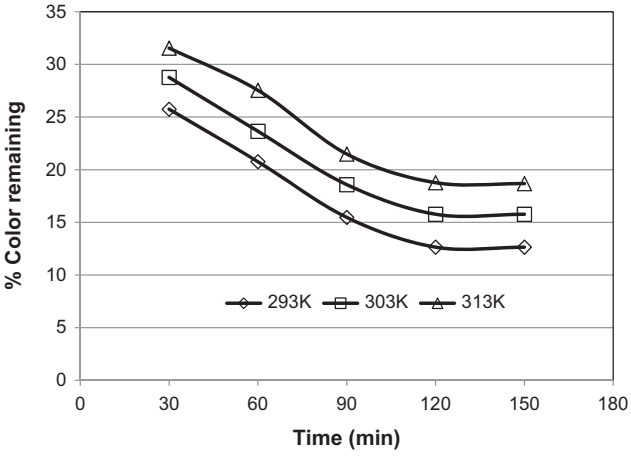

Fig. 2. Effect of temperature on spentwash adsorption using fly ash.
Notes: Conditions: pH 7, particle size BSS # –150 + 200, dosage = 10 g, time = 150 min, dilution = 10%.

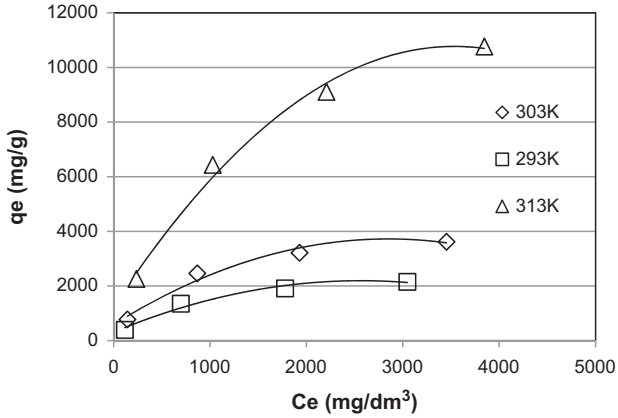

Fig. 3. Predicted q_e for different temperatures of adsorption studies using modified Langmuir isotherm.
Notes: Conditions: pH 7, particle size BSS # –150 + 200, dosage = 10 g, time = 150 min.

Table 1
Modified Langmuir model equations for various temperatures

Temperature (K)	Predictive correlations
293	$q_e = \frac{.00155 \times 293^{1.4641}}{1 + .00155 \times C_e}$
303	$q_e = \frac{.00155 \times 303^{1.4641}}{1 + .00155 \times C_e}$
313	$q_e = \frac{.0008 \times 313^{1.67419}}{1 + .0008 \times C_e}$

3.3. Studies on effect of initial concentration of solute on spentwash adsorption

The batch adsorption studies were performed at different initial concentrations of melanoidin pigments with 10 g of fly ash adsorbent to analyze the effect of initial concentration of solute. It was observed that the concentration of solute decreases with time due to increased rate of adsorption of pigments on fly ash. The rate of change of concentration was negligible after a period of 100 min as observed from Fig. 4 and hence it is reasonable to assume that adsorption has reached equilibrium after a period of 150 min. It was observed that initial concentration controlled the rate of concentration drop at initial stages of experiments but after some time the rate is constant for all experiments with different initial concentrations. This is because when the initial concentration is large the deviation of initial concentration from equilibrium concentration is higher which results in large concentration gradient and increased rate of mass transfer.

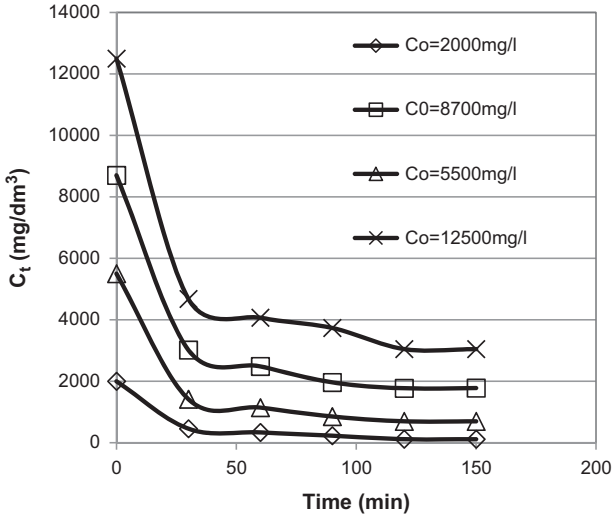

Fig. 4. Effect of initial concentration of solute on spentwash adsorption.
Notes: Conditions: pH 7, particle size BSS # –150 + 200, dosage = 10 g, time = 150 min.

3.4. Mass transfer studies

The diffusion takes place in non-homogeneous media and the effective diffusivity considers both pore diffusion and surface diffusion. The effective diffusivity is represented by the following equation [10]:

$$D_{\text{eff}} = D_{\text{P}} + \rho_{\text{p}} D_{\text{s}} \frac{\partial Y}{\partial C} \tag{5}$$

In this equation the derivative term $\partial Y/\partial C$ represents the slope of isotherm. The values of the effective diffusivity were evaluated at different dilutions based on above equation as shown in Table 2. The effective diffusivity depends on initial concentration of solution and the predictive correlation for effective diffusivity is represented as follows:

$$D_{\text{eff}} = a\, C_{\text{o}}^{b}$$

The predictive correlations for effective diffusivity of sorption of distillery spentwash on fly ash adsorbent at different temperatures are given in Table 3. The effect of initial concentrations of spentwash at different temperatures on effective diffusivity is shown in Fig. 5 and it is observed that the effective diffusivity remained constant at higher concentrations but decreased with temperature at dilute concentrations. This is because at high solute concentration the surface diffusion coefficient is negligible and diffusion is controlled by pore diffusivity which is independent of temperature but at reduced solute concentration the surface diffusion becomes dominant.

Table 2
Values of effective diffusivity at different initial concentrations for sorption of spentwash on fly ash adsorbent based on mass transfer model

Temperature (K)	Dilution (%)	D_{eff} (m^2/s)
293	5	6.45×10^{-7}
	10	2.40×10^{-7}
	15	1.59×10^{-7}
	20	1.36×10^{-8}
303	5	5.90×10^{-7}
	10	2.00×10^{-7}
	15	1.63×10^{-7}
	20	1.28×10^{-8}
313	5	5.59×10^{-7}
	10	2.21×10^{-7}
	15	1.68×10^{-7}
	20	1.30×10^{-8}

Table 3
Predictive correlations for effective diffusivity of sorption of distillery spentwash on fly ash adsorbent at different temperatures based on mass transfer model

Temperature (K)	Predictive correlations
293	$D_{\text{eff}} = 0.384\ C_{\text{o}}^{9.17 \times 10^{-3}}$
303	$D_{\text{eff}} = 0.404\ C_{\text{o}}^{5.57 \times 10^{-4}}$
313	$D_{\text{eff}} = 0.179\ C_{\text{o}}^{0.386}$

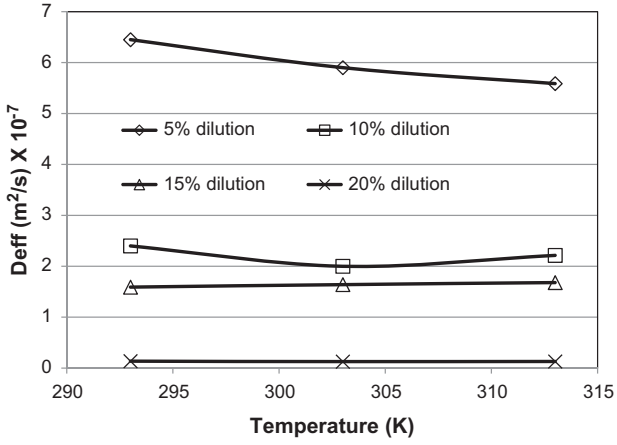

Fig. 5. Effect of initial concentrations of spentwash and temperatures on effective diffusivity based on mass transfer model.

3.5. Optimization of contact time in batch adsorbers

The two batch adsorbers arranged in series were considered and their contact times were optimized based on following assumptions:

(1) The mass of adsorbent in each adsorber is same.
(2) The adsorbent is not recycled which means the initial concentration of adsorbate in the adsorbent is zero.
(3) The solid and liquid phases are in equilibrium in both adsorbers.

The contact time depends on initial concentration of adsorbate in the second adsorber and hence to optimize the contact time a feasible range of initial concentration values for second adsorber were found.

3.5.1. Determination of lower bound of C_{O2}

It was assumed based on unreacted shrinking core model that the capacity factor must be less than 1 and this assumption can be used to find the lower bound of C_{O2}. The concentration in the second adsorber cannot be more than the equilibrium concentration of the first adsorber and hence these two inequalities can be solved to obtain lower bound of concentration. The equations for these inequalities are listed below:

$$\frac{Sq_e}{VC_{min1}} \leq 1.0 \tag{6}$$

$$\frac{VC_0 - Sq_e}{V} \leq C_{min2} \tag{7}$$

In the above equations C_{min1} and C_{min2} represents the boundary values of individual solutions for each inequality. The actual lower bound can be obtained by taking the maximum of these values.

$$C_{O2min} = \max\left[C_{min1}, C_{min2}\right]$$

3.5.2. Determination of upper bound of C_{O2}

The maximum amount of material that can be adsorbed by the adsorbent in the second stage is equal to equilibrium concentration times the adsorbent mass. This condition can be mathematically expressed as:

$$VC_{max1} - VC_2 \leq Sq_e \tag{8}$$

The initial concentration in second adsorber cannot exceed the initial concentration in first adsorber:

$$C_{max1} \leq C_0 \tag{9}$$

Solving the above equations the upper and lower bounds of C_{O2} was obtained. The average of these two bounds was taken as the mean value of initial concentration.

$$C_{O2} = 0.5(C_{min} + C_{max}) \tag{10}$$

The set of C_{O2} values for different volumes of first adsorber was obtained as shown in Fig. 6 and it can be observed that for the given range of volumes the optimal values of C_{O2} is equal to the lower bound values. The lower and upper bound curves merge at pinch point volume of 3 m^3 which is the optimal value as shown in Fig. 6.

3.5.3. Contact time optimization of batch adsorbers

The optimal contact time for the system was estimated using the analytical solution of the unreacted shrinking core model given below [10]:

$$\tau = \frac{1}{6C_H}\left\{\ln\left[\frac{x^3 + a}{1 + a^3}\right]^{\left(2B-\left(\frac{1}{a}\right)\right)} + \ln\left[\left[\frac{x + a}{1 + a}\right]\right]^{3/a}\right\} + \frac{1}{a\sqrt{3}C_H}\left\{\arctan\left[\frac{2 - a}{a\sqrt{3}}\right] - \arctan\left[\frac{2x - a}{\sqrt{3}}\right]\right\} \tag{11}$$

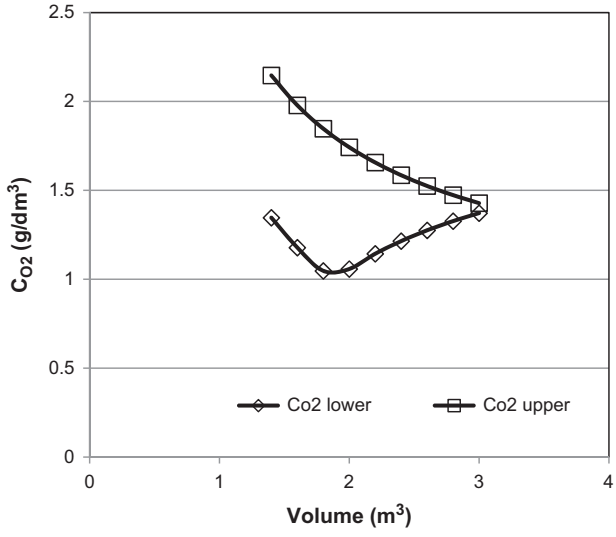

Fig. 6. Effect of volume of liquid phase on initial concentration of second adsorber using unreacted shrinking core model.

The optimal contact time obtained was plotted against the corresponding C_{O2} values as shown in Fig. 7 and it can be observed that the optimal contact time for first adsorber decreased with an increase in C_{02} values because adsorbent in the first adsorber adsorbs less quantity of adsorbate. In the second adsorber the contact time increased with increase in C_{02} values. The sum of optimal contact times of first and second adsorber gives the overall contact time of 40 min for 1.5 mg/dm^3 C_{02} value as shown in Fig. 7.

3.6. Determination of adsorption parameters for continuous adsorption using film pore diffusion model

The film pore diffusion model used assumes that mass transfer occurs in a thin film adjacent to the adsorbent surface and drop in concentration occurs across the thickness of film and film diffusion remains the rate-controlling step. The final equations used to predict the values of theoretical concentration of adsorption are described below in two sections [24,25].

For section 1:

$$\zeta = h_{11} - h_{21} \tag{12}$$

$$\text{with } h_{11} = \frac{1}{6}\ln\frac{\left(1 - X_2^3\right)^{2B}\left(X_2^2 + X_2 + 1\right)}{\left(1 - X_2^2\right)} - \frac{1}{\sqrt{3}}\tan^{-1}\frac{\left(2X_2 + 1\right)}{\sqrt{3}} \tag{13}$$

$$\text{where } B = 1 - \frac{1}{B_i} \tag{14}$$

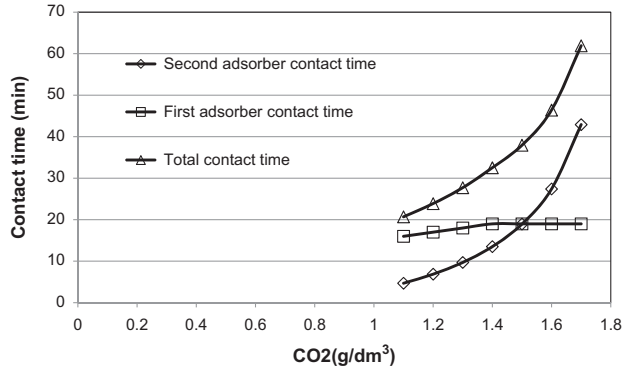

Fig. 7. Contact time optimization of two batch adsorbers using unreacted shrinking core model.

$$X_2 = (1 - \eta(0,\tau)\xi)^{(1/3)} \tag{15}$$

$$\text{and } h_{21} = \frac{1}{6}\ln\frac{\left(1 - X_0^3\right)^{2B}\left(X_0^2 + X_0 + 1\right)}{\left(1 - X_0^2\right)} - \frac{1}{\sqrt{3}}\tan^{-1}\frac{\left(2X_0 + 1\right)}{\sqrt{3}} \tag{16}$$

$$X_0 = (1 - \eta(0,\tau))^{(1/3)} \tag{17}$$

For section 2:

$$\zeta = h_{12} - h_{22} \tag{18}$$

$$\text{with } h_{12} = \frac{1}{6}\ln\frac{\left(1 - X_2^3\right)^{2B}\left(X_2^2 + X_2 + 1\right)}{\left(1 - X_2^2\right)} - \frac{1}{\sqrt{3}}\tan^{-1}\frac{\left(2X_2 + 1\right)}{\sqrt{3}} \tag{19}$$

$$X_2 = (1 - \xi)^{(1/3)} \tag{20}$$

$$\text{and } h_{22} = \tau_1 - \tau - \frac{\pi}{18}\sqrt{3} \tag{21}$$

The equations were solved using MATLAB software to determine the external mass transfer coefficient, effective diffusivity, and bed capacity. The external mass transfer coefficient was determined using various correlations listed in Table 4 and for all these correlations the mass transfer coefficients were determined and an average of these values was taken as the representative value for k.

The Biot number is the ratio of inter particle diffusion to intra particle diffusion as given below:

$$B_i = \frac{kR}{D_{eff}} \tag{22}$$

The Biot number calculated is larger than 10^9 and hence external mass transfer controls the rate of adsorption process. The adsorbent bed capacity has significant effect on diffusion as it determines the residence time of adsorbate in adsorber column. The adsorbent bed capacity at 303 K determined from Langmuir adsorption model for different initial concentrations at 2000, 5,500, 8,700, and 12,500 mg/ml are 69.26, 114.41, 143.64, and 172 mg/g, respectively. The adsorbent bed capacity was larger for continuous adsorption process in comparison to batch adsorption due to difference in residence time of adsorbate in the bed.

Table 4
External mass transfer coefficient values for adsorption of melanoidin pigments on fly ash adsorbent

Refs.	Empirical correlation	Range of validity	k (cm/s)
[26]	$Sh = 5.4\ Re^{(1/3)}\ Sc^{(1/4)}$	$0.04 < Re < 30$	51.74
[27]	$Sh = 4.3\ Re^{0.35}\ Sc^{1/4}$	$0.1 < Re < 3$	40.74
[28]	$Sh = 4.58\ Re^{(1/3)}\ Sc^{(1/3)}$	$0.4 < Re < 10$	43.40
[29]	$Sh = (1.09/\varepsilon)\ Re^{(1/3)}\ Sc^{(1/3)}$	$0.016 < Re < 55$	17.04
[30]	$Sh = 2.4\ \varepsilon^{0.66}\ Re^{(0.34)}\ Sc^{(1/3)}$	$0.04 < Re < 52$	2.399
[31]	$Sh = (1.13/\varepsilon)\ Re^{(0.21)}\ Sc^{(1/3)}$	$Re < 10$	17.215
[32]	$Sh = 1.85((1-\varepsilon)/\epsilon^2)Re^{(1/3)}Sc^{(1/3)}$	$Re/(1-\varepsilon) < 10$	52.56
[33]	$Sh = Re^{(0.28)}\ Sc^{(1/3)}$	$Re < 10$	5.4
[34]	$Sh = 2 + 1.58\ Re^{(0.4)}\ Sc^{(1/3)}$	$0.001 < Re < 5.8$	98.72
[35]	$Sh = 0.644\ Re^{(1/2)}\ Sc^{(1/3)}$	$Sc < 12{,}000$	3.65

Note: Flow rate =1L/hr, Initial concentration = 2,000 mg/ml.

Table 5
Effective diffusion coefficient of melanoidin adsorption onto fly ash adsorbent in continuous column using film pore diffusion model

Bed height (cm)	D_{eff} (cm^2/s) × 10^{-11}
5	4.75
10	4.99
15	5.23
20	5.54

Notes: Initial concentration = 2,000 mg/ml, Flow rate = 1 L/hr.

The effective diffusion coefficient of continuous adsorption process was determined using film pore diffusion model for each value of concentration and from these set of values the effective diffusion coefficient for which the error between theoretical values and experimental values were least was selected as the best fit value. The values of effective diffusion coefficient at different bed heights are shown in Table 5 for adsorption of melanoidin pigments onto fly ash adsorbent column. The values of effective diffusivity at 5, 10, 15, and 20 cm bed height are 4.75×10^{-11}, 4.99×10^{-11}, 5.23×10^{-11}, and 5.54×10^{-11} cm^2/s, respectively.

4. Conclusion

The biopolymeric pigments in distillery spentwash were removed using coal fly ash as adsorbent in batch and continuous adsorbers. The optimization of contact time of adsorption in two adsorbers were determined using unreacted shrinking core model and the total optimal contact time was 40 min for 1.5 mg/dm^3 initial concentration in second adsorber for liquid-phase volume of 3 m^3. The film pore diffusion model was used to determine the external mass transfer coefficient, effective diffusion coefficient, and bed capacity of continuous adsorption process. The effective diffusivity at 5, 10, 15, and 20 cm fly ash adsorbent are 4.75×10^{-11}, 4.99×10^{-11}, 5.23×10^{-11}, and 5.54×10^{-11} cm^2/s, respectively. The values of adsorbent bed capacity for different initial concentrations at 303 K were determined.

Nomenclature

q_e	—	equilibrium concentration in solid phase (mg/g)
K_L and a_L	—	Langmuir isotherm constants
b and n	—	modified Langmuir isotherm constants that considers the energy of adsorption
D	—	diffusivity (m^2/s)
ρ_p	—	density of adsorbent particles (kg/m^3)
Y	—	solid-phase concentration (mg/g)
C	—	solution concentration (mg/dm^3)
a and b	—	correlation parameters for effective diffusivity
S	—	adsorbent weight (kg)
V	—	volume of liquid phase (dm^3)
m_s	—	concentration of sorbent in liquid phase (mg/L)
% R_t	—	percentage color removal
k	—	external mass transfer coefficient (cm/s)
B_i	—	Biot number, dimensionless
R	—	radius of adsorbent particle (cm)
Sh	—	Sherwood number
Re	—	Reynolds number
ξ	—	dimensionless concentration $\xi = \frac{C_t}{C_o}$
ζ	—	dimensionless bed height $\zeta = \frac{mD_{eff}}{\vartheta \rho_s R^2} Z$
τ	—	dimensionless time $\tau = \frac{C_o D_{eff} t}{\rho_p q_e R^2}$
η	—	dimensionless bed capacity, $\eta = \frac{q}{q_e}$
τ_1	—	dimensionless time required for the top most layer to reach equilibrium

m	—	adsorbent mass (g)
ρ_s	—	solution density (kg/m^3)
Z	—	bed height (m)
ϑ	—	volumetric flow rate (L/h)

Subscripts

e	—	equilibrium
O	—	initial
t	—	time
min	—	minimum
max	—	maximum
1	—	first stage
2	—	second stage
eff	—	effective
p	—	pore
s	—	surface

References

[1] B.L. Wedzicha, M.T. Kaputo, Melanoidins from glucose and glycine: Composition, characteristics and reactivity towards sulphite ion, Food Chem. 43 (1992) 359–367.

[2] P. Manisankar, C. Rani, S. Viswanathan, Effect of halides in the electrochemical treatment of distillery effluent, Chemosphere 57(8) (2004) 961–966.

[3] W. Chu, Dye removal from textile dye wastewater using recycled alum sludge, Water Res. 35(13) (2001) 3147–3152.

[4] A.K. Verma, P. Bhunia, R.R. Dash, Decolorization and COD reduction efficiency of magnesium over iron based salt for the treatment of textile wastewater containing diazo and anthraquinone dyes, Int. J. Chem. Sci. Eng. 6(6) (2012) 1278–1286.

[5] V.S. Mane, I.D. Mall, V.C. Srivastava, Use of bagasse fly ash as an adsorbent for the removal of brilliant green dye from aqueous solution, Dyes Pigm. 73 (2007) 269–278.

[6] S. Wang, Y. Boyjoo, A. Choueib, A comparative study of dye removal using fly ash treated by different methods, Chemosphere 60 (2005) 1401–1407.

[7] S. Kara, C. Aydiner, E. Demirbas, M. Kobya, N. Dizge, Modeling the effects of adsorbent dose and particle size on the adsorption of reactive textile dyes by fly ash, Desalination 212 (2007) 282–293.

[8] A. Adamczuk, D. Kołodyńska, Equilibrium, thermodynamic and kinetic studies on removal of chromium, copper, zinc and arsenic from aqueous solutions onto fly ash coated by chitosan, Chem. Eng. J. 274 (2015) 200–212.

[9] G. McKay, Analytical solution using a pore diffusion model for a pseudoirreversible isotherm for the adsorption of basic dye on silica, AIChE J. 30 (1984) 692.

[10] B. Chen, C.W. Hui, G. McKay, Film-pore diffusion modeling and contact time optimization for the adsorption of dyestuffs on pith, Chem. Eng. J. 84 (2001) 77–94.

[11] K.K. Choy, G. McKay, J.F. Porter, A film-pore surface diffusion model for the adsorption of acid dyes on activated carbon, Adsorption 7 (2001) 231–247.

[12] S. Dutta, J.K. Basu, R.N. Ghar, Studies on adsorption of p-nitrophenol on charred saw-dust, Sep. Purif. Technol. 21 (2001) 227–235.

[13] G. McKay, The adsorption of dyestuffs from aqueous solution using activated carbon: Analytical solution for batch adsorption based on external mass transfer and, Chem. Eng. J. 27 (1983) 187.

[14] G. Mckay, M. El-Geundi, M.M. Nassar, Pore diffusion during the adsorption of dyes onto bagasse pith, Process Saf. Environ. Prot. 74 (1996) 277.

[15] N. Pinto, E. Graham, Application of the shrinking core model for predicting protein adsorption, React. Polym. 5 (1987) 49.

[16] R. Krishna Prasad, S.N. Srivastava, Sorption of distillery spentwash onto fly ash: Kinetics, mechanism, process design and factorial design, J. Hazard. Mater. 161 (2009) 1313–1322.

[17] D. Francisca Kalavathi, L. Uma, G. Subramanian, Degradation and metabolization of the pigment-melanoidin in distillery effluent by the marine cyanobacterium *Oscillatoria boryana* BDU 92181, Enzyme Microb. Technol. 29 (2001) 246–251.

[18] G. Christoskovas, L.D. Lazarov, Electrochemical method for purification and discoloration of cellulose paper industry wastewaters, Environ. Prot. Eng. 14 (2006) 69–76.

[19] P.K. Chaudhari, I.M. Mishra, S. Chand, Decolourization and removal of chemical oxygen demand (COD) with energy recovery: Treatment of biodigester effluent of a molasses-based alcohol distillery using inorganic coagulants, Colloids Surf. A: Physicochem. Eng. Aspects 296 (2007) 238–247.

[20] P.R. Kasten, L. Lapidus, N.R. Amundson, Mathematics of Adsorption in Beds. V. Effect of Intra-particle Diffusion in Flow Systems in Fixed Beds, J. Phys. Chem. 56 (1952) 683–688.

[21] C. Raghukumar, G. Rivonkar, Decolorization of molasses spentwash by the white rot fungus *Flavodon flavus*, isolated from a marine habitat, Appl. Microbiol. Biotechnol. 55 (2001) 510–514.

[22] M. Mohammadi, M.J. Ameri Shahrabi, M. Sedighi, Comparative study of linearized and non-linearized modified Langmuir isotherm models on adsorption of Asphaltene onto mineral surfaces, Surf. Eng. Appl. Electrochem. 48(3) (2012) 234–243.

[23] S. Sohn, D. Kim, Modification of Langmuir isotherm in solution systems—Definition and utilization of concentration dependent factor, Chemosphere 58 (2005) 115–123.

[24] G. McKay, M.J. Bino, Adsorption of pollutants onto activated carbon in fixed beds, J. Chem. Technol. Biotechnol. 37 (1987) 81–93.

[25] C.K. Danny, J.F. Porter, G. McKay, Film pore diffusion model for the fixed bed sorption of copper and cadmium ions onto bone char, Water Res. 35 (2001) 3876–3886.

[26] F. Coeuret, Percolating porous electrode—I Mass transfer in fixed bed, Electrochim. Acta 21 (1976) 185–193.

[27] H. Olive, G. Lacoste, Application of volumetric electrodes to the recuperation of metals in industrial effluents—I. Mass transfer in fixed beds of spherical conductive par, Electrochim. Acta 24 (1979) 1109–1114.

[28] A.J. Karabelas, T.H. Wegner, T.J. Hanratty, Use of asymptotic relations to correlate mass transfer data in packed beds, Chem. Eng. Sci. 26 (1971) 1581–1589.
[29] E.J. Wilson, C.J. Geankoplis, Liquid mass transfer at very low Reynolds number in packed beds, Ind. Eng. Chem. Fund. 5(1) (1966) 9–14.
[30] J.E. Williamson, K.E. Bazaire, C.J. Geankoplis, Liquid-phase mass transfer at low reynolds numbers, Ind. Eng. Chem. Fundam. 2(2) (1963) 126–129.
[31] S. Kumar, S.N. Upadhyay, V.K. Mathur, Low reynolds number mass transfer in packed beds of cylindrical particles, Ind. Eng. Chem. Process Des. Develop. 16(1) (1977) 1–8.
[32] T. Kataoka, H. Yoshida, K. Ueyama, Mass transfer in laminar region between liquid and packing material surface in packed bed, J. Chem. Eng. Jpn. 5(2) (1972) 34–38.
[33] P.N. Dwivedi, S.N. Upadhyay, Particle-fluid mass transfer in fixed and fluidized beds, Ind. Eng. Chem. Process Des. Develop. 16(2) (1977) 157–165.
[34] H. Ohashi, T. Sugawara, K.I. Kikuchi, H. Konno, Correlation of liquid-side mass transfer coefficient for single particles and fixed beds, J. Chem. Eng. Jpn. 14 (6) (1981) 433–438.
[35] V. Gnielinski, Equations for calculation of heat and mass transfer in perfused ballasting of spherical particles at medium and high Peclet numbers, Verfahrenstechnik 12(6) (1978) 363–367.